



ARCHIVES
 of
 FOUNDRY ENGINEERING

DOI: 10.1515/afe-2017-0080

Published quarterly as the organ of the Foundry Commission of the Polish Academy of Sciences



ISSN (2299-2944)

Volume 17

Issue 2/2017

227 – 239

Effect of Degassing Treatment on the Interfacial Reaction of Molten Aluminum and Solid Steel

T. Triyono ^{a,*}, N. Muhayat ^a, A. Supriyanto ^a, L. Lutiyaatmi ^b^a Universitas Sebelas Maret, Jl. Ir. Sutami 36 A, 57126 Surakarta, Indonesia^b Politeknik Manufaktur Ceper Batur, Ceper, Klaten 57465 Jawa, Indonesia

* Corresponding author. E-mail address: triyonomesin@uns.ac.id

Received 10.03.2017; accepted in revised form 25.04.2017

Abstract

The gas porosity is one of the most serious problems in the casting of aluminum. There are several degassing methods that have been studied. During smelting of aluminum, the intermetallic compound (IMC) may be formed at the interface between molten aluminum and solid steel of crucible furnace lining. In this study, the effect of degassing treatment on the formations of IMC has been investigated. The rectangular substrate specimens were immersed in a molten aluminum bath. The holding times of the substrate immersions were in the range from 300 s to 1500 s. Two degassing treatments, argon degassing and hexachloroethane tablet degassing, were conducted to investigate their effect on the IMC formation. The IMC was examined under scanning electron microscope with EDX attachment. The thickness of the IMC layer increased with increasing immersion time for all treatments. Due to the high content of hydrogen, substrate specimens immersed in molten aluminum without degasser had IMC layer which was thicker than others. Argon degassing treatment was more effective than tablet degassing to reduce the IMC growth. Furthermore, the hard and brittle phase of IMC, FeAl₃, was formed dominantly in specimens immersed for 900 s without degasser while in argon and tablet degasser specimens, it was formed partially.

Keywords: Degassing treatment, Crucibles furnace, Intermetallic compounds, Molten aluminum, Solid steel

1. Introduction

Aluminum castings are widely used in cars for engine blocks, heads pistons, rocker covers, inlet manifold, deferential casings, steering boxes, brackets, wheels, etc. The potential for further use of aluminum in automotive applications is considerable due to the demands for reduced automobile weight to obtain improved fuel efficiency [1]. The common conclusion of the several researches in the field of aluminum casting showed that the gas porosity is one of the most serious problems in the casting of aluminum [1-7]. It is generally caused by the evolution of gasses during the casting and solidification process. The gasses may be the result of a reaction between the casting sand or mold and the metal, or they

may result from the evolution of gasses dissolved in the liquid metal during solidification. Porosity is detrimental to the mechanical properties and corrosion resistance of Aluminum castings. It is dominantly affected by the hydrogen gas which is always present in the smelting process. The solubility of the hydrogen gas in the extraordinary solid decreases as compared to in the liquid metal. It makes the hydrogen gas trapped during solidification and leads the porosity [3]. Thus, the degassing, the elimination of the hydrogen in molten aluminum is crucial for producing high-quality castings. There are several degassing methods that have been studied in the past few decades, including re-melting degassing [3], vacuum degassing [8], ultrasonic degassing [4,9], spray degassing [10,11], rotary impeller

degassing [12] and tablet degassing by hexachloroethane (C_2Cl_6) [13].

The presence of hydrogen gas can interfere the atomic cohesive force of the host materials. The atomic cohesive force is needed to increase the interatomic attractive force. It means that hydrogen gas reduces the atomic bonding strength of the material [14]. On the microscopic scale, hydrogen gas affects grain boundary segregation and then affects the mechanism of diffusion [15]. The higher content of hydrogen gas in the substrate, the lower of bonding strength, the more segregation of grain boundary and the easier diffusion of elements. The diffusion is the key role in compounds formation including the intermetallic compounds (IMC) formation. It is well known that in aluminum casting, the IMC (Intermetallic compound) may be formed at the interface between molten aluminum and solid steel of crucible furnace lining because the operating temperature is $660^\circ C$ to $760^\circ C$ and holding time is in the range of 5-30 minutes. Based on the phase diagram of Fe-Al as seen in Fig. 1, there are several types of intermetallic compounds, among others: Fe_3Al , $FeAl$, $FeAl_2$, Fe_2Al_5 and $FeAl_3$. There have been several investigations on the intermetallic compound analysis at the interface when molten aluminum comes in contact with solid steel in many cases of joining and casting [16-24]. They have conclusively reported the natures of intermetallic compounds which brittle and hard.

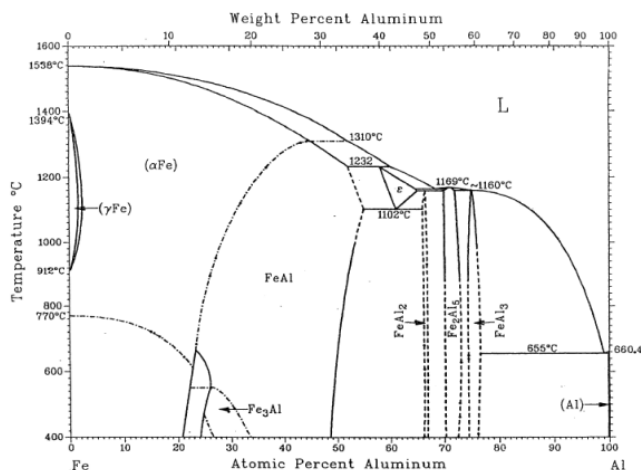


Fig. 1. Fe-Al Equilibrium phase diagram¹¹

Due to their natures, intermetallic compounds formation gradually erodes steel walls or lining of the crucible furnace and leads to damage the furnace when melting process is done. It means that intermetallic compounds formation is detrimental to a life time of crucible furnace. Degassing treatment will affect the behavior of molten aluminum, including gas bubble evolution [2,3], steady state time and hydrogen content [4]. It is predicted that they will affect diffusion of an iron atom into aluminum and

vice versa, and finally affect the intermetallic compounds formation because it is dependent on diffusion coefficients between the steel substrate and the molten aluminum [18]. The research problem is whether the degassing treatment affects the intermetallic compound formation or not and how the mechanism of the degassing in influencing the IMC formation.

In this study, the effects of degassing treatment on the Fe-Al intermetallic compound formation at the interface between molten aluminum and solid steel of crucible furnace lining were investigated to understand the possibility of crucible furnace failure caused by the inappropriate degassing method. Two degassing methods in the aluminum casting process, argon and tablet degassing, were evaluated and compared to process without degassing treatment.

2. Experimental Procedure

2.1. Materials

Materials in this study represented the melting process of aluminum in conventional crucible furnace so that the materials were steel as the substrate sample and aluminum as a molten bath. The substrate samples were machined from the steel of conventional crucible furnace lining. Aluminum AA5083 was used in this study. The chemical composition of test materials is shown in Table 1. Ultrahigh purity argon with a purity of 99% and hexachloroethane tablet (C_2Cl_6) were used to degas the molten aluminum.

2.2. Methods

A 4000 g aluminum plat was cut and melted in a conventional crucible furnace to make a molten aluminum bath with a volume of about 1500 cc. Two degassing treatments, argon degassing and hexachloroethane tablet (C_2Cl_6) degassing, were conducted to investigate their effect on the intermetallic compounds formation. Aluminum melting without degassing treatment was also performed, and its behavior was compared to that of aluminum melting with degassing treatments. The experimental set-up of these three aluminum meltings is shown in Fig. 2, where 1 is a furnace, 2 is melting furnace, 3 is wood charcoal, 4 is molten aluminum, 5 is steel coupons, 6 is thermocouple and 7 is degassing gas. A temperature range from $700^\circ C$ to $800^\circ C$ was maintained during each test. In argon degassing process, argon was injected to molten aluminum bath at the rate of $0.1 m^3/h$.

Table 1.

The chemical composition (wt-%) of test materials.

element	Fe	C	Si	Cr	Mn	P	S	Mo	Al	Mg	Ni
Steel	98.600	0.217	0.209	0.022	0.463	0.042	0.031	0.005	-	-	-
AA5083	0.230	-	0.050	0.015	0.825	-	-	-	94.550	3.580	0.020

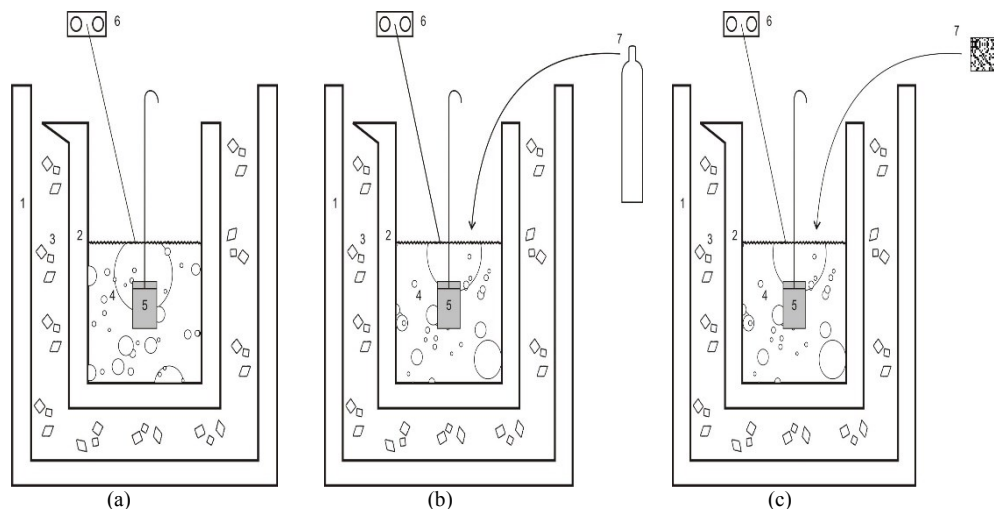


Fig. 2. Schematic diagram of the experimental set-up, consists of three processes: (a) without degasser, (b) Argon degasser and (c) Tablet degasser

The rectangular substrate specimens having 50x50x6 mm in dimension were finished using a sand paper of grade 1000 and washed in alcohol before immersion in the aluminum bath. They were then immersed in a molten aluminum bath. The holding times of the substrate immersions were in the range from 300 s to 1500 s. After that, the immersed specimens were cooled to room temperature in air.

The immersed specimens were cut perpendicular to the thickness and then polished using sand paper of grades 240-1200. Due to nature of dissimilar metals bonding, two stages etchant were used for etching. In the first stage of etching, a 90% fluoride acid solution was used to reveal microstructure of aluminum and intermetallic compound. The microstructure of steel side was revealed using a solution of 5 ml nitric acids in 95 ml alcohol. The etching process was done at room temperature for 3 s. To observe the intermetallic compound, etched specimens were examined under scanning electron microscope (TESCAN Vega3 LMU) with EDX (OXFORD INCA Energy 250) attachment.

Microhardness tests were subjected across the interface to further clarify the intermetallic compound using a load of 200 g. The hardness profiles were defined by indenting from the aluminum layer to the steel substrate in 50 μm increments. The effect of neighboring indentations was eliminated by spaced analysis points.

3. Results and Discussion

Figure 3 shows micrographs of cross sections of the Intermetallic Compound (IMC) layers of steel substrates immersed in a molten aluminum bath for 300 s without degasser, with argon degasser and with tablet degasser respectively. It is seen that the IMC was formed in all of the specimens. The IMC of without degasser and with tablet degasser specimen were thicker than that of with argon degasser specimen.

It seems that hydrogen gas plays an important role in the formation of IMC. When substrates were immersed in the molten aluminum bath, hydrogen gas dissolved in molten aluminum easily due to its high solubility. It dissolved in all parts of the molten aluminum including the interface between it and the solid steel substrates. During smelting process, dissolved hydrogen gas in molten aluminum is going through the surface of solid steel substrates. It will reduce the bond strength between materials atoms [14] and segregate the grain boundary [15] of both aluminum and solid steel surface. This condition coupled with high temperature during smelting will facilitate diffusion between Al atom of molten aluminum and Fe atom of solid steel surface. Due to the atomic radius of Al atom is smaller than that of Fe atom, where atomic radius of Al atom is 118 pm while that of Fe atom is 156 pm [25], Al atom tends to penetrate to solid steel surface so that IMC was formed at solid steel surface and grew into steel substrates. It appeared in the specimen without degasser as seen in Fig. 3(a).

In argon degassing, when argon gas is injected, the molten aluminum becomes turbulent, and as it travels, hydrogen is collected and removed to and from the surface. Moreover, the stream produced by injecting argon gas speeds up the process [4]. It will reduce the hydrogen content in molten aluminum. Decreasing hydrogen content in molten aluminum is not detrimental to bonding strength of material, so diffusion rate between Al atom and Fe atom is low, and finally, IMC layer didn't grow as seen in Fig. 3(b). Furthermore, the IMC of the tablet degasser specimen (Fig. 3(c)) was almost similar to that of without degasser specimen although its IMS was thinner than IMC of without degasser specimen. The tablet degasser composed of chlorine and fluorine containing salts. If it is inserted into the molten aluminum, it will react with aluminum and produce aluminum chloride gas and aluminum fluoride gas in the form of vacuum bubbles where their pressure is less than 1 atm. Dissolved hydrogen gas cannot get out because the pressure inside the molten aluminum is less than 1 atm, while the outside pressure is 1 Atm [7]. Shih and Wen (2005) [26] said that if the molten

aluminum is in a vacuum environment, the hydrogen partial pressure will drop dramatically to near zero. In this case, it diffuses from the molten aluminum into the bubbles. The bubbles

escape from the molten aluminum, and the hydrogen gas is then removed by the exhausting system.

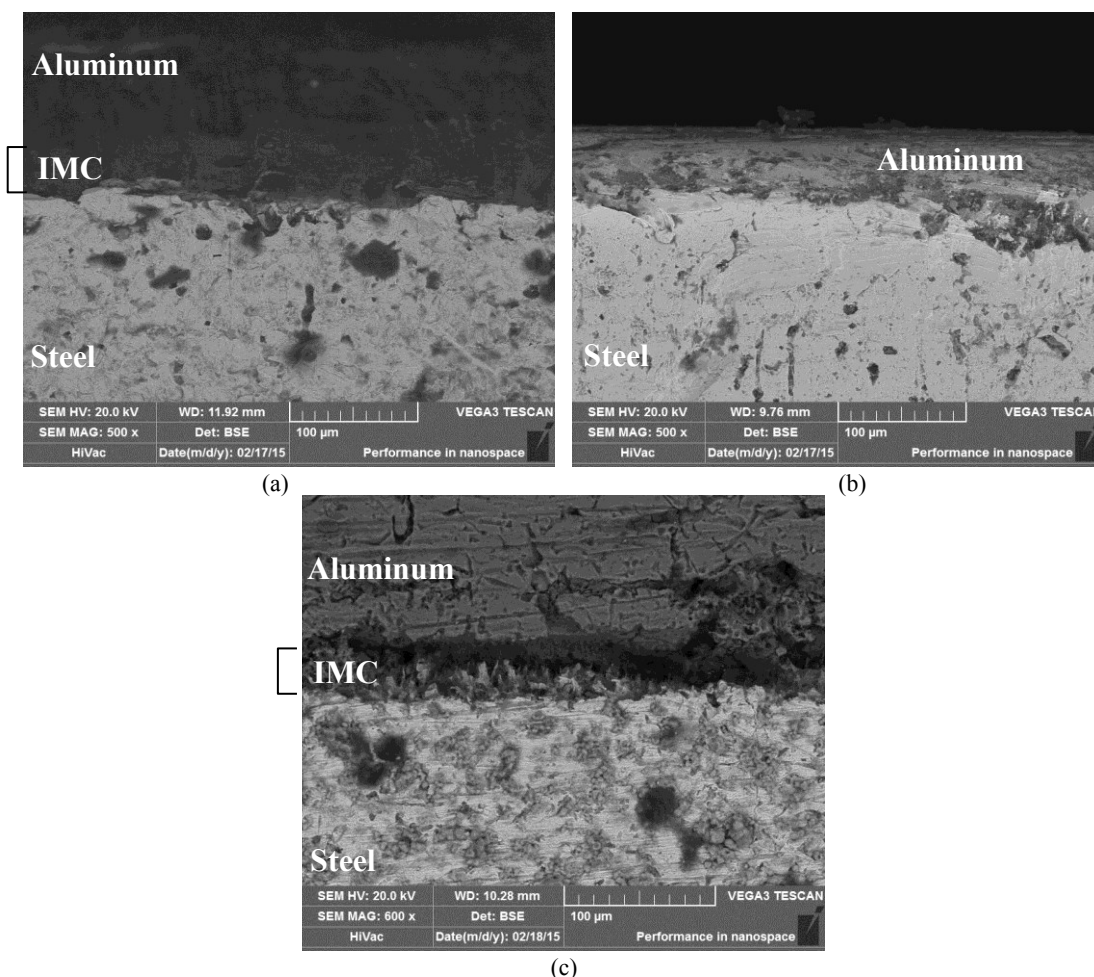


Fig. 3. Intermetallic compound morphology of specimens immersed for 300 s (a) without degasser (b) with argon degasser and (c) with tablet degasser

The effect of degassing treatment on the thickness of IMC at interface Aluminum-steel will be more evident in specimens with longer immersion. Fig. 4, 5, 6 and 7 display the IMC layers of steel substrates immersed in a molten aluminum bath without degasser, with argon degasser and with tablet degasser for 600 s, 900 s, 1200 s and 1500 s respectively. For all conditions of molten aluminum, the thickness of the IMC layer increased with increasing immersion time. Based on the SEM images, the IMC thickness of each condition was measured and summarized in a graph as shown in Fig. 8. It shows the comparison of IMC thicknesses for all conditions. It is well known that IMC thickness (X) depends on immersion time (t) and temperature (T). It is described by the equations $X=(2Kt)^{0.5}$ and $K=K_0 \exp(-Q/RT)$ where K is growth constant, K_0 is constant, R is the gas constant, and Q is the activation energy for growth of layer [19]. When the immersion time is short, Al atoms concentration at the interface is very small, and the interface tends to form Al-Fe solid solution.

However, when the immersion time is extended, Al atoms concentration at the interface of steel substrate increases gradually with the increasing of immersion time. At a certain time, Al atoms and Fe atoms begin to react to form Al-Fe compound at the interface, and according to Zhang et al. [27], it is 4.3 s. The longer immersion time, the more the Al-Fe compound.

From Fig. 8, for all immersion time, it is seen that the IMC in without degasser specimen was thickest while that in argon degasser was thinnest. The IMC thickness of tablet degasser specimen was between thickness of without degasser and argon degasser specimens. Argon gas was more effective than a tablet to reduce hydrogen in a molten aluminum bath. The growth of IMC thickness is related to the amount of hydrogen in molten aluminum. Argon degasser can inhibit IMC growth effectively due to its success to drive hydrogen in molten aluminum. It means that the argon degasser can extend aluminum casting time without worrying about IMC growth. Consequently, the operator has more

time to wait aluminum for melting completely and ready to be poured without forming IMC so the steel wall of crucible will not

be eroded.

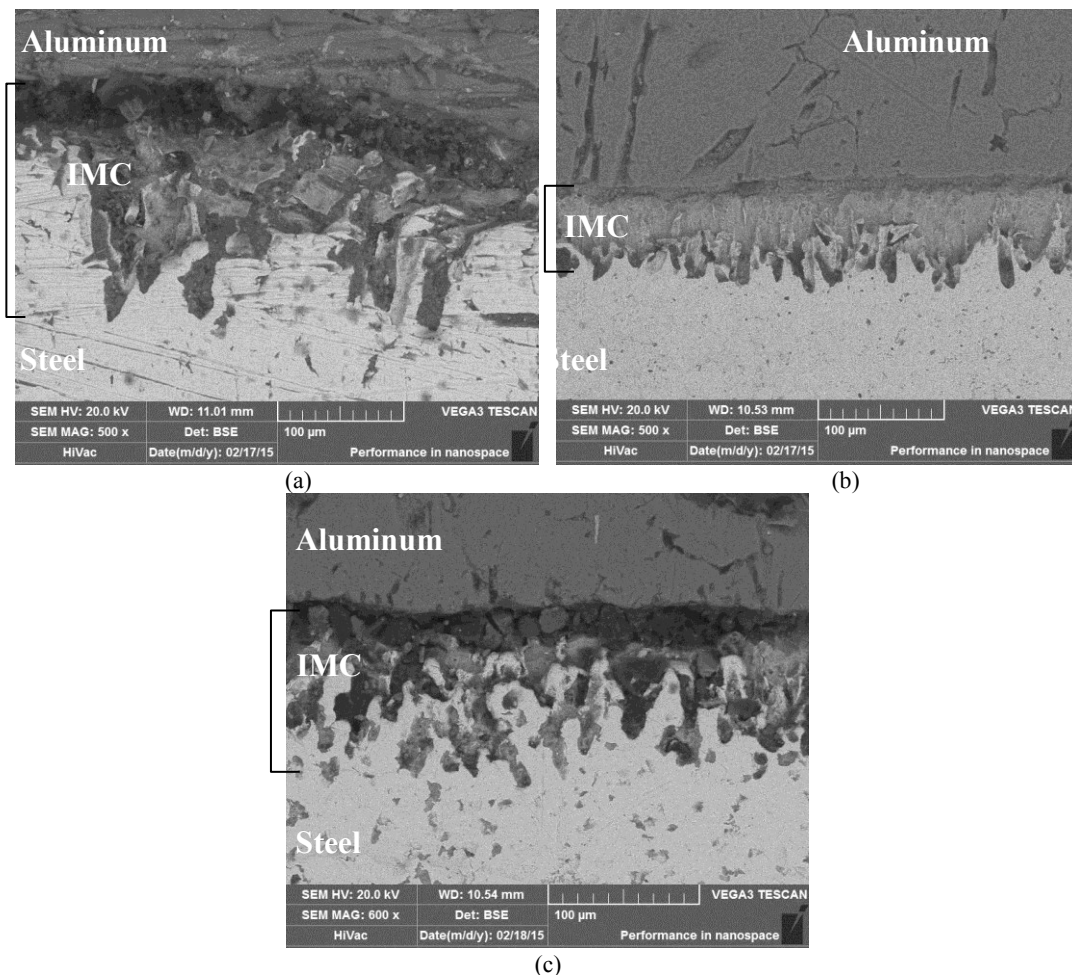


Fig. 4. Intermetallic compound morphology of specimens immersed for 600 s (a) without degasser (b) with argon degasser and (c) with tablet degasser

Degassing treatment affected not only the thickness of IMC at the interface Al-Steel but also the phase transformation of IMC, especially for specimens with a long immersion time. For all degassing treatments, based on the EDS spectra of selected points, the FeAl phase was dominantly formed at the interface Al-Steel of specimens immersed until for 600 s as seen in Fig. 9, Fig. 10 and Fig. 11, and it will be formed various phases of IMC after 900 s of immersion depending on the degassing treatments as seen in Fig. 12 and Fig. 13.

The IMC types of selected points in Fig. 12 were summarized in Table 2. It is seen that hard and brittle phase of IMC, FeAl₃, was formed dominantly in specimens immersed for 900 s without degasser. The facility of Aluminum diffusion facilitated the formation of this phase. In the tip and base of tongue structure,

the phase Fe₂Al₅ was formed. In specimens with degasser both argon degasser and tablet degasser, the FeAl₃ phase was formed partially in the base of tongue structure due to retardation of Aluminum diffusion.

When immersion time was extended until 1200 s, in without degasser specimens, Fe atoms diffused into the FeAl₃ phase and then Fe₂Al₅ was formed at the interface of Steel-Aluminum. Fe atoms diffused continuously, and then FeAl was formed. It was identified that the growth of all intermetallic compound layers was controlled by the diffusion of Fe atoms into the Al-rich intermetallic layers [18]. Due to retardation of diffusion rate, the Al-rich intermetallics, FeAl₃ and Fe₂Al₅ were still formed in the specimens with argon and tablet degasser. The IMC types of specimens immersed for 1200 s were summarized in Table 3.

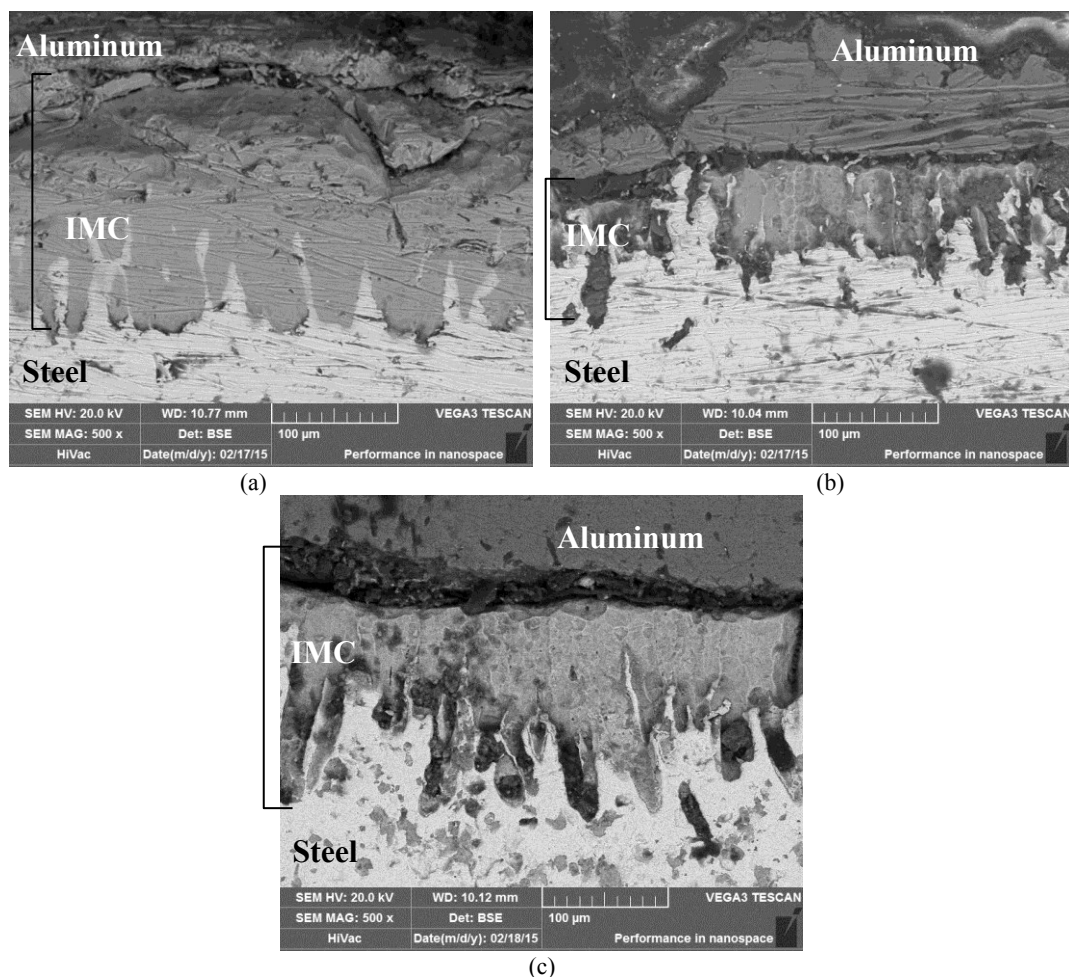


Fig. 5. Intermetallic compound morphology of specimens immersed for 900 s (a) without degasser (b) with argon degasser and (c) with tablet degasser

In this study, from SEM images and EDS spectra, it is known that all of the specimens do not undergo reaction with oxygen. It means that there is no corrosion at the interface between steel substrate and aluminum. It is well known that aluminum is one of the least noble of the common commercial metals. During melting of aluminum, dissolve oxygen will react with molten aluminum to form unstable alumina. The stability of alumina increases as the temperature decreases, and the solubility of oxygen in molten

aluminum decrease with temperature as well, so reaction automatically occurs in aluminum as it cools and solidifies [28-29]. Consequently, oxygen cannot reach the interface between steel substrate and aluminum so there is no corrosion on the surface of steel substrate. This principle is used in the process of steel corrosion protection by using sprayed aluminum coating [30-31].

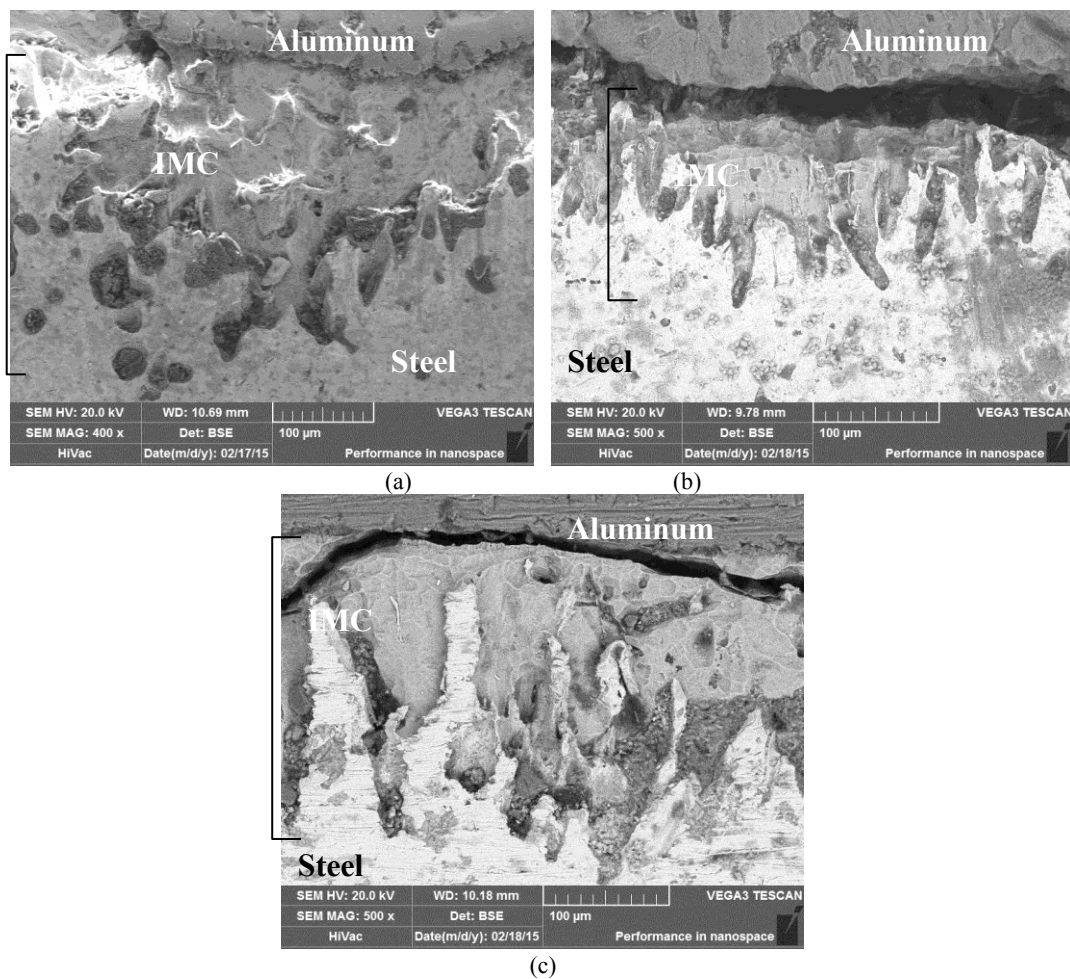


Fig. 6. Intermetallic compound morphology of specimens immersed for 1200 s (a) without degasser (b) with argon degasser and (c) with tablet degasser

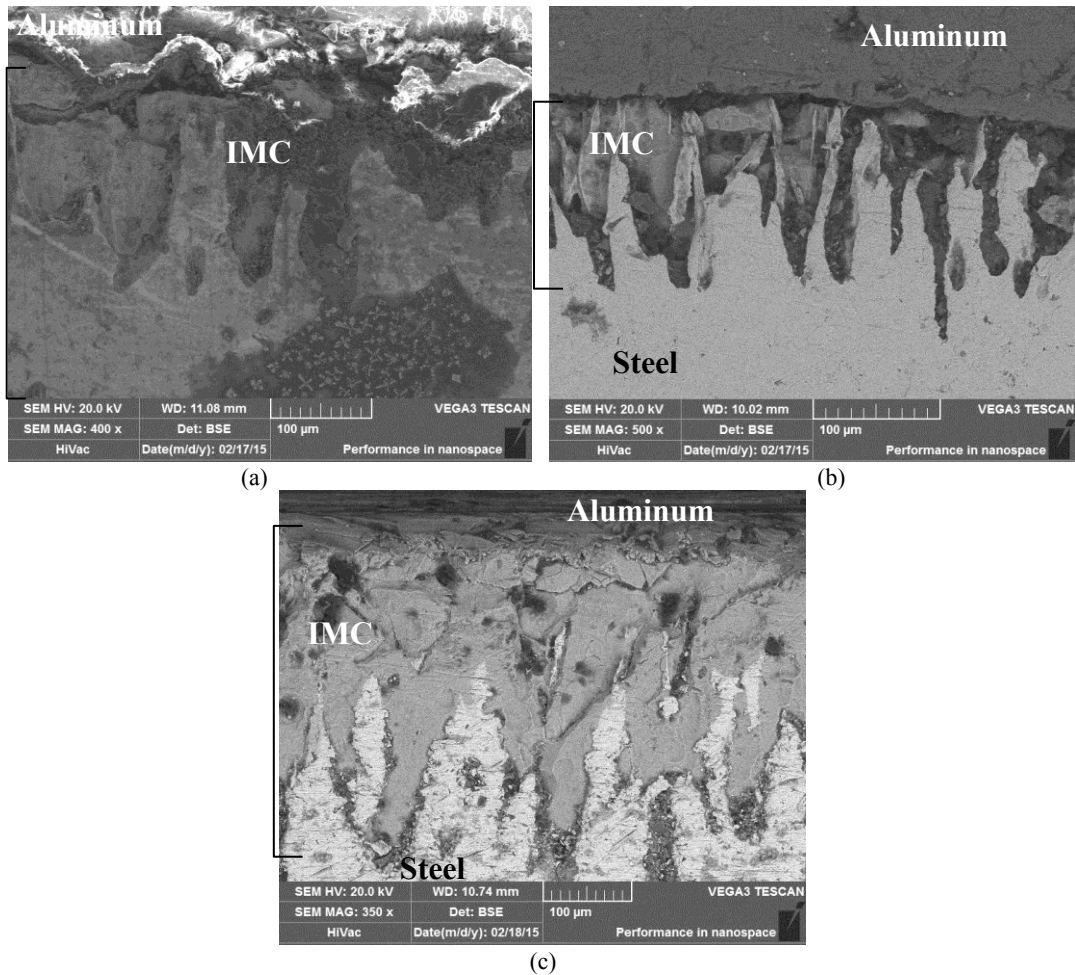


Fig. 7. Intermetallic compound morphology of specimens immersed for 1500 s (a) without degasser (b) with argon degasser and (c) with tablet degasser

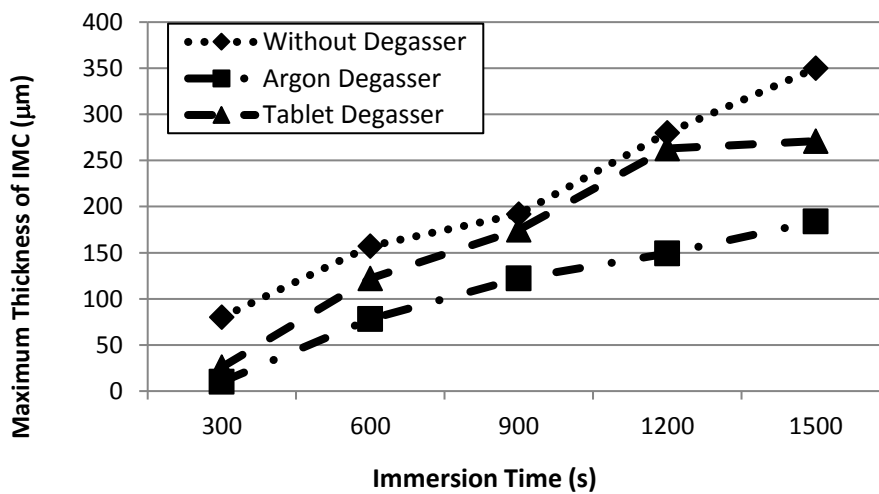


Fig. 8. Thickness of Intermetallic Compound (IMC) layer depending on immersion time

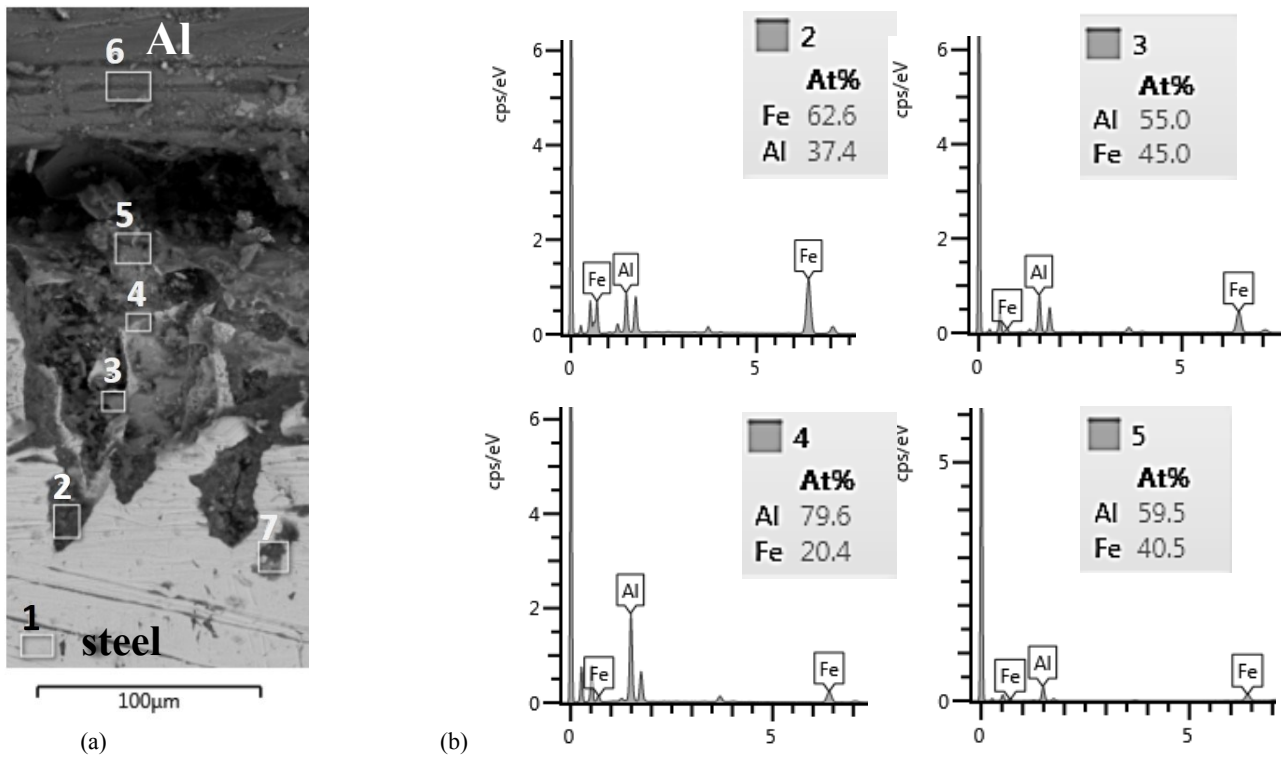


Fig. 9. (a) EDX-analyzed spots at the interface Al-Steel of specimens immersed for 600 s without degasser associated with Fig. 4(a), (b) EDS spectra of selected points

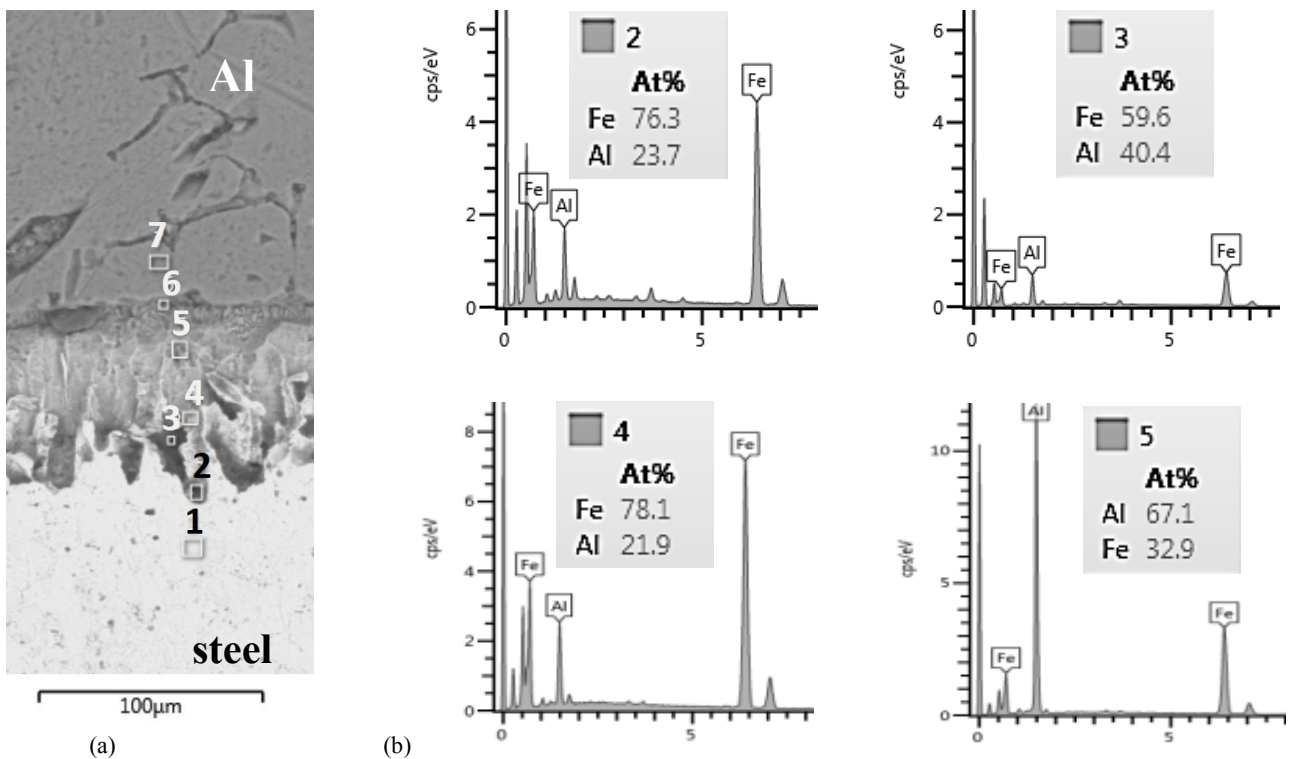


Fig. 10. (a) EDX-analyzed spots at the interface Al-Steel of specimens immersed for 600 s with argon degasser associated with Fig. 4(b), (b) EDS spectra of selected points

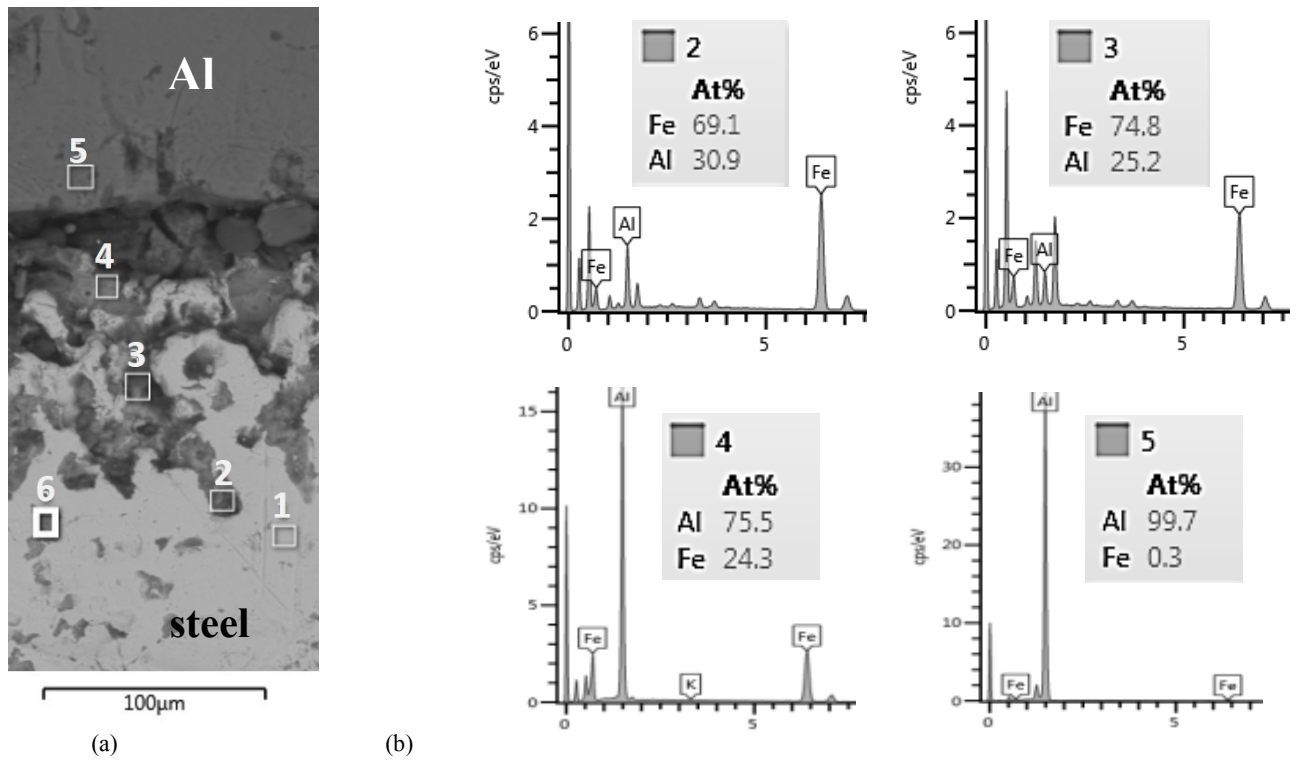


Fig. 11. (a) EDX-analyzed spots at the interface Al-Steel of specimens immersed for 600 s with tablet degasser associated with Fig. 4(c), (b) EDS spectra of selected points

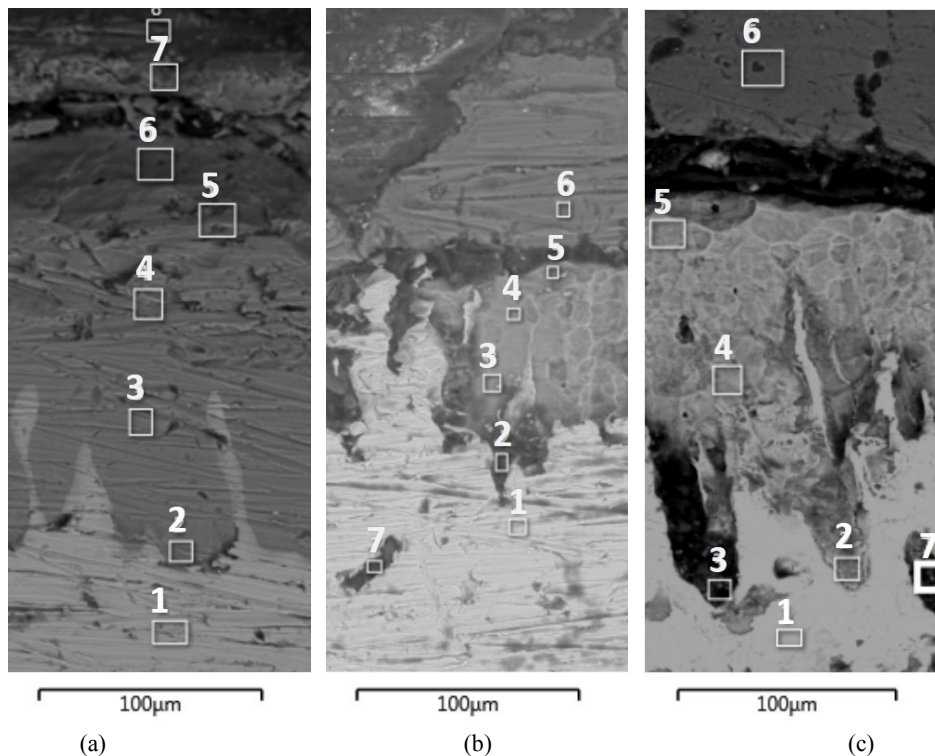


Fig. 12. EDX-analyzed spots at the interface Al-Steel of specimens immersed for 900 s (a) without degasser (b) with argon degasser and (c) with tablet degasser associated with Fig. 5.

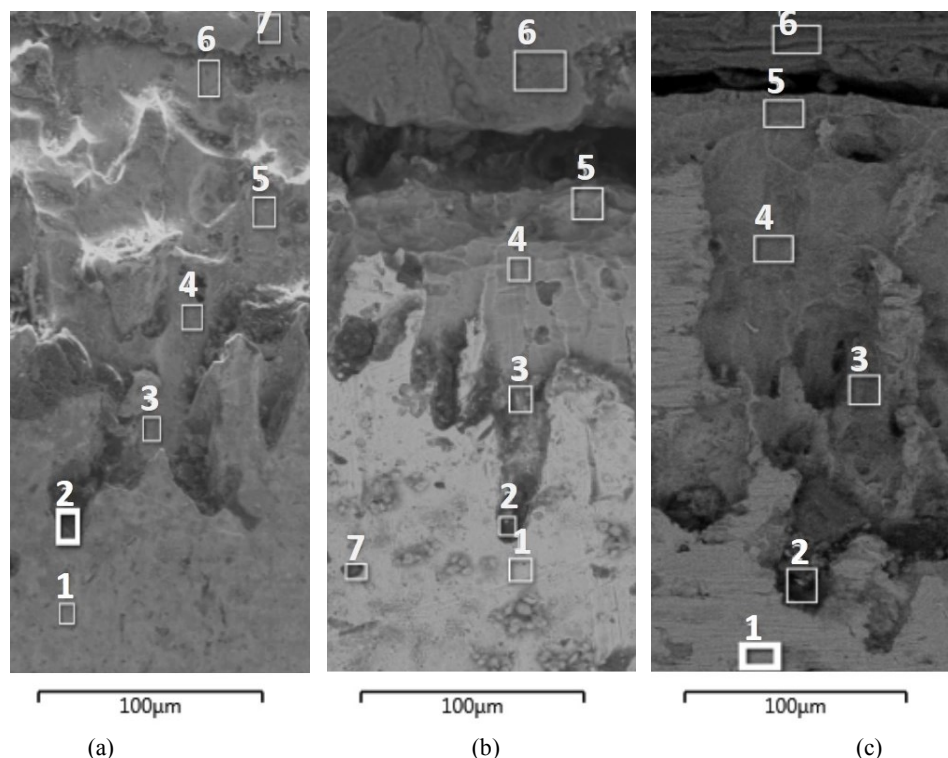


Fig. 13. EDX-analyzed spots at the interface Al-Steel of specimens immersed for 1200 s (a) without degasser (b) with argon degasser and (c) with tablet degasser associated with Fig. 6.

Table 2.

IMC types based on EDS spectra of selected points in Fig. 12

Point no.	without degasser			argon degasser			tablet degasser		
	Fe	Al	IMC	Fe	Al	IMC	Fe	Al	IMC
1	98.9	1.1	Fe	99.4	0.6	Fe	99.1	0.9	Fe
2	30.2	69.8	Fe ₂ Al ₅	47.1	52.9	FeAl	72.8	27.2	FeAl
3	25.6	74.4	FeAl ₃	31.2	68.8	FeAl ₂	58.2	41.8	FeAl
4	26.4	73.6	FeAl ₃	25.0	75.0	FeAl ₃	27.0	73.0	Fe ₂ Al ₅
5	23.2	76.8	FeAl ₃	51.3	48.7	FeAl	25.1	74.9	FeAl ₃
6	22.9	77.1	FeAl ₃	0.2	99.8	Al	0.3	99.7	Al
7	27.5	72.5	Fe ₂ Al ₅	93.5	6.5	Fe	49.8	50.2	FeAl
8	1.7	98.3	Al						

Table 3.

IMC types based on EDS spectra of selected points in Fig. 13

Point no.	without degasser			argon degasser			tablet degasser		
	Fe	Al	IMC	Fe	Al	IMC	Fe	Al	IMC
1	82.1	17.9	Fe	95.6	4.4	Fe	98.9	1.1	Fe
2	74.9	25.1	FeAl	69.7	30.3	FeAl	69.0	31.0	FeAl
3	55.5	44.5	FeAl	68.3	31.7	FeAl	57.2	42.8	FeAl
4	27.8	72.2	Fe ₂ Al ₅	24.3	75.7	FeAl ₃	26.9	73.1	Fe ₂ Al ₅
5	27.1	72.9	Fe ₂ Al ₅	22.5	77.5	FeAl ₃	26.6	73.4	Fe ₂ Al ₅
6	15.7	84.3	Al	1.5	98.5	Al	0.3	99.7	Al
7	20.5	79.5	Al	48.9	51.1	FeAl			

4. Conclusion

The thickness of the IMC layer increased with increasing immersion time for all treatments. For longer immersion time, Fe in steel and Al in aluminum alloys have sufficient time to react, form IMC and grow toward steel. Tongue-like IMC will appear after an immersion time of 600 s. Besides immersion time, the content of hydrogen gas in molten aluminum also plays an important role in the formation of IMC. Due to the high content of hydrogen, substrate specimens immersed in molten aluminum without degasser had the thickest IMC layer. Degassing treatment can reduce the content of hydrogen gas in molten aluminum and then inhibit the IMC growth. Argon degassing treatment was more effective than tablet degassing to reduce the IMC growth. Furthermore, the hard and brittle phase of IMC, FeAl₃, was formed dominantly in specimens immersed for 900 s without degasser while in argon and tablet degasser specimens, it was formed partially. Due to nature of FeAl₃, it leads the crucible wall be eroded easily.

Acknowledgments

This research was financially supported by Sebelas Maret University through PNPB 2015 grant with contract no. 698 /UN27/PN/2015.

References

- [1] Raiszadeh, R. & Griffiths, W.D. (2010). The behavior of double oxide film defects in liquid Al alloys under atmospheric and reduced pressures. *Journal of Alloys and Compounds*. 491, 575-580.
- [2] Ren, Y., Ma, W., Wei, K., Yu, W., Dai, Y., & Morita, K. (2014). Degassing of aluminum alloys via the electromagnetic directional solidification. *Vacuum*. 109, 82-85.
- [3] Zhao, L., Pan, Y., Liao, H. & Wang Q. (2012). Degassing of aluminum alloys during re-melting. *Materials Letters*. 66, 328-331.
- [4] Haghayeghi, R., Bahai, H. & Kapranos, P. (2012). Effect of ultrasonic argon degassing on dissolved hydrogen in aluminum alloy. *Materials Letters*. 82, 230-232.
- [5] Dispinar, D., Akhtar, S., Nordmark, A., Di Sabatino, M. & Arberg, L. (2010). Degassing, hydrogen and porosity phenomena in A356. *Materials Science and Engineering A*. 527, 3719-3725.
- [6] Eisaabadi, B.G., Davami, P., Kim, S.K. & Varahram, N. (2012). Effects of hydrogen and oxides on tensile properties of Al-Si-Mg cast alloys. *Materials Science and Engineering A*. 552, 36-47.
- [7] Zeng, J., Gu, P. & Wang, Y. (2012). Investigation of Inner Vacuum Sucking method for degassing of molten aluminum, *Materials Science and Engineering B*. 177, 1717-1720.
- [8] Xu, H., Meek, T.T. & Han, Q. (2007). Effects of ultrasonic field and vacuum on degassing of molten aluminum alloy. *Materials Letters*. 61, 1246-1250.
- [9] Eskin, G.I. (1998). Prospects of ultrasonic (cavitational) treatment of the melt in the manufacture of aluminum alloy products. *Metallurgist*. 42, 284-291.
- [10] Wu, R., Qu, Z., Sun, B. & Shu, D. (2007). Effects of spray degassing parameters on hydrogen content and properties of commercial purity aluminum, *Materials Science and Engineering A*. 456, 386-390.
- [11] Warke, V.S., Tryggvason, G. & Makhlof, M.M. (2005). Mathematical modeling and computer simulation of molten metal cleansing by the rotating impeller degasser: Part I. Fluid flow. *Journal of Materials Processing Technology*. 168, 112-118.
- [12] Wang, L., Guo, E., Huang, Y. & Lu, B. (2009). Rotary impeller refinement of 7075Al alloy. *Rare Metals*. 28, 309-312.
- [13] Samuel, A.M. & Samuel, F.H. (1992). Various aspects involved in the production of low-hydrogen aluminium castings. *Journal of Materials Science*. 27, 6533-6563.
- [14] Oriani, R.A. (1993). The Physical and Metallurgical Aspects of Hydrogen in Metals. in ICCF4. Fourth International Conference on Cold Fusion. Lahaina, Maui: Electric Power Research Institute 3412 Hillview Ave., Palo Alto, CA 94304.
- [15] Song, R.G., Tseng, M.K., Zhang, B.J., Liu, J., Jin, Z.H. & Shin, K.S. (1996). Grain boundary segregation and hydrogen-induced fracture in 7050 Aluminium alloy. *Acta Metall.* 44, 3241-3248.
- [16] Shahverdi, H.R., Ghomashchi, M.R., Shabestari, S., & Hejazi, J. (2002). Microstructural analysis of interfacial reaction between molten aluminum and solid iron. *Journal of Materials Processing Technology*. 124, 345-352.
- [17] Chen, C.M. & Kovacevic, R. (2004). Joining of Al 6061 alloy to AISI 1018 steel by combined effects of fusion and solid state welding. *International Journal of Machine Tools & Manufacture*. 44, 1205-1214.
- [18] Kobayashi, S. & Yakou, T. (2002). Control of intermetallic compound layers at interface between steel and aluminum by diffusion-treatment. *Materials Science and Engineering A*. 338, 44-53.
- [19] Qiu R., Shi, H., Zhang, K., Tu, Y., Iwamoto, C. & Satonaka, S. (2010). Interfacial characterization of joint between mild steel and aluminum alloy welded by resistance spot welding. *Materials Characterization*. 61, 684-688.
- [20] Tanaka, T., Morishige, T. & Hirata, T. (2009). Comprehensive analysis of joint strength for dissimilar friction stir welds of mild steel to aluminum alloys. *Scripta Materialia*. 61, 756-759.
- [21] Ogura, T., Saito, Y., Nishida, T., Nishida, H., Yoshida, T., Omichi, N., Fujimoto, M. & Hirose, A. (2012). Partitioning evaluation of mechanical properties and the interfacial microstructure in a friction stir welded aluminum alloy/stainlesssteel lap joint. *Scripta Materialia*. 66, 531-534.
- [22] Schimek, M., Springer, A., Kaierle, S., Kracht, D. & Wesling, V. (2012). Laser-welded dissimilar steel-aluminum seams for automotive lightweight construction. *Physics Procedia*. 39, 43-50.
- [23] Uematsu, Y.; Tokaji, K., Tozaki, Y. & Nakashima, Y. (2010). Fatigue behaviour of dissimilar friction stir spot weld between A6061 and SPCC welded by a scrolled groove shoulder tool. *Procedia Engineering*. 2, 193-201.

- [24] Yajiang, L., Juan, W., Yansheng, Y. & Haijun, M. (2005). Diffusivity of Al and Fe near the diffusion bonding interface of Fe₃Al with low carbon steel. *Bull. Mater. Sci.* 28(1), 69-74.
- [25] Clementi, E., Raimondi, D.L., Reinhardt, W.P. (1967). Atomic Screening Constants from SCF Functions. II. Atoms with 37 to 86 Electrons, *J. Chem. Phys.* 47, 1300.
- [26] Shih, T-S, & Wen, K-Y. (2005). Effects of Degassing and Fluxing on the Quality of Al-7%Si and A356.2 Alloys. *Materials Transactions.* 46(2), 263 - 271.
- [27] Zhang, P. Du, Y., Xing, S., Zhang, L., Zeng, D., Cui, J. & Ba, L. (2002). Influence of Diffusion Time on Steel-Aluminum Solid to Liquid Bonding Interfacial Structure, *J. Mater. Sci. Technol.* 18(05), 468-470.
- [28] Schiesinger, M.E. (2014). *Aluminum Recycling*, CRC Press, Taylor and Francis Group, Boca Raton.
- [29] Hatch, J.E. (2005). *Aluminum, Properties and Physical Metallurgy*, American Society for Metals, tenth printing
- [30] Lee, H-S., Singh, J.K., Ismail, M.A. & Bhattacharya, C. (2016). Corrosion Resistance Properties of Aluminum Coating Applied by Arc Thermal Metal Spray in SAE J2334 Solution with Exposure Periods. *Metals.* 6(55), 1-15.
- [31] Esfahani, E.A., Salimijazi, H., Golozar, M.A., Mostaghimi, J. & Pershin, L. (2012). Study of Corrosion Behavior of Arc Sprayed Aluminum Coating on Mild Steel. *Journal of Thermal Spray Technology.* 21(6), 1195-1202